Polymer Chemistry

ROYAL SOCIETY OF CHEMISTRY

PAPER

View Article Online
View Journal | View Issue

Check for updates

Cite this: *Polym. Chem.*, 2025, **16**, 1478

Organocatalyzed photoredox radical cyclopolymerization of methacrylate- and acrylamide-crotonate hybrid monomers†

Gaoyuan Yu,‡[a] Yong-Le Tian,‡[b] Ke Li[c] and Dian-Feng Chen *[c]

Received 30th November 2024,
Accepted 21st February 2025

DOI: 10.1039/d4py01369g

rsc.li/polymers

Cascade bond-forming polymerizations have emerged as a powerful strategy for the synthesis of polymeric materials with advanced structures and properties. Among these, radical cyclopolymerization is one of the most extensively studied methodologies, although it still faces several challenges, including low cyclization rates, unwanted crosslinking, and lack of spatiotemporal control. Herein, we report the design and synthesis of methacrylate- and acrylamide-crotonate hybrid monomers, which undergo a visible light-driven, organocatalyzed photoredox ATRP-type cyclopolymerization. This approach eliminates crosslinking and proceeds through a sophisticated sequence of intramolecular cyclization and intermolecular propagation, yielding diverse homopolymers and block copolymers with cyclic repeating units. Additionally, factors influencing the control over polymer chain growth, such as light intensity and additives, are explored.

Open Access Article. Published on 21 February 2025. Downloaded on 1/23/2026 4:09:17 AM.
This article is licensed under a Creative Commons Attribution-NonCommercial 3.0 Unported Licence.

Introduction

The merger of reversible-deactivation radical polymerization (RDRP) with visible-light photocatalysis has been recognized as a mild and versatile strategy for synthesizing polymers with diverse structures and functionalities.[1–7] This approach not only imparts excellent control over polymer chain growth, tailoring the molecular weights (MWs) and narrowing the molecular weight distributions,[8] but also provides unique spatiotemporal control which enables a broad scope of applications ranging from photolithography to 3D manufacturing.[9–12] Among the numerous mechanisms employed in photocontrolled RDRP, atom transfer radical polymerization (ATRP) is one of the most extensively studied controlled radical polymerization methodologies.[6,13] In contrast to the early ATRP examples mediated by Cu(I)[14] or Ru(II)[15] complexes under thermal conditions, the development of photocontrolled ATRP has focused on two dimensions: sustainable photoredox processes and an expanded monomer scope. To address concerns about transition metal contaminations, considerable efforts have been directed toward the development of efficient photocatalysts (PCs), shifting from metal complexes[16–22] to metal-free systems. As such, a variety of purely organic molecules, including perylene,[23,24] phenothiazines,[25–28] dihydrophenazines,[29,30] phenoxazines,[31,32] carbazoles,[33] thienothiophenes,[34] dihydroacridines,[35] and oxygen-/sulfur-doped polycyclic arenes,[36,37] have proven effective and practical for organocatalyzed ATRP (O-ATRP), yielding well-defined polymers with high chain-end fidelity and a controlled topology. On the other hand, methacrylates have dominated the research of O-ATRP, while progress involving other vinyl monomers (*e.g.*, acrylates,[27,28,35,38] acrylamides,[39,40] acrylonitrile,[26,41] and styrene[23–33]) remains limited. Expanding the scope of polymerizable monomers, particularly those with intriguing polymerizability profiles, is highly desirable for further advancing this field.

In contrast to conventional single-reactivity monomers, multi-functionalized molecules hold the potential for cascade reactions in polymerizations, leading to advanced polymers with unique structures and properties.[42–45] A premier example is the radical cyclopolymerization of diene monomers, where sequential intramolecular cyclization and propagation ideally proceed to afford linear polymers with cyclic repeating units (Fig. 1a).[46] In the realm of free-radical cyclopolymerization, various divinyl monomers have been designed to (a) enable the direct preparation of functional polymeric materials, such as poly(diallyldimethylammoniumchloride)[47] and its copolymers with acrylamide for water treatment, and (b) address the alternation challenge in copolymerization of two distinct vinyl monomers through an alternating intra-intermolecular chain mechanism. Additionally, conventional nitroxide-mediated

[a]*Department of Thyroid and Breast Surgery, Affiliated Anhui Provincial Hospital, Anhui Medical University, Hefei 230032, China*
[b]*College of Chemistry and Chemical Engineering, Qingdao University, Qingdao 266071, China*
[c]*Hefei National Research Center of Physical Sciences at the Microscale and Department of Polymer Science and Engineering, University of Science and Technology of China, Hefei, Anhui 230026, China. E-mail: cdf@ustc.edu.cn*
†Electronic supplementary information (ESI) available. See DOI: https://doi.org/10.1039/d4py01369g
‡These authors contributed equally to this work.

This journal is © The Royal Society of Chemistry 2025

Open Access Article. Published on 21 February 2025. Downloaded on 1/23/2026 4:09:17 AM.
This article is licensed under a Creative Commons Attribution-NonCommercial 3.0 Unported Licence.

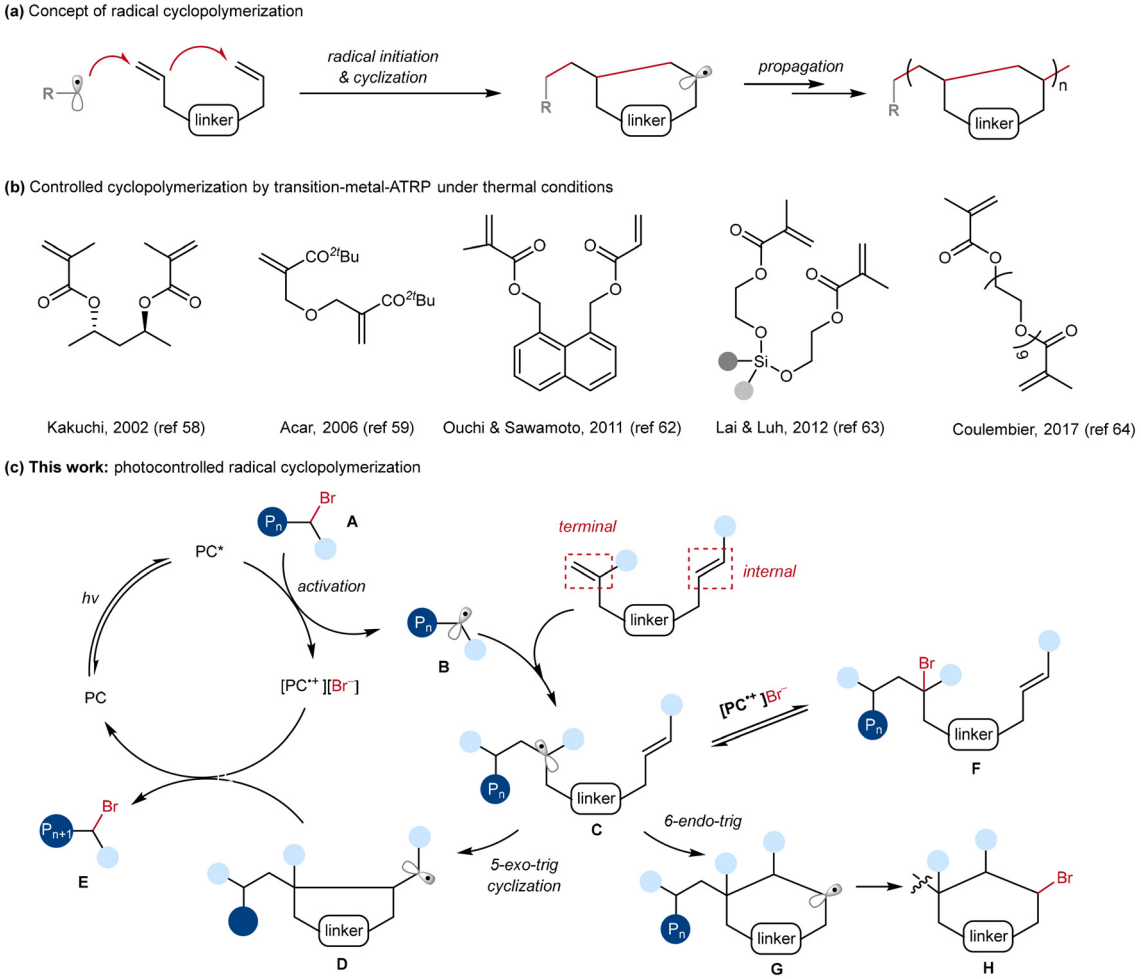

Fig. 1 (a) Concept of radical cyclopolymerization. (b) Cyclopolymerization using transition-metal-based ATRP technology. (c) Photocontrolled radical cyclopolymerization in this work.

radical polymerization (NMP),[48] reversible addition-fragmentation chain transfer (RAFT),[49–57] and ATRP[58–61,62–64] techniques have been applied to radical cyclopolymerization, offering precise control over MWs, dispersities, and chain-end livingness, which enables sequence-defined copolymerization (Fig. 1b). Despite these advancements, a photocontrolled radical cyclopolymerization has yet to be realized, likely due to long-standing problems, such as low cyclization rates and inevitable crosslinking, which complicate the process and hinder the effective control by a photocatalyst.

We hypothesized that a vinyl monomer bearing a pendent internal alkene functionality would help minimize these unwanted side reactions in radical cyclopolymerizaiton. As depicted in Fig. 1c, a highly reducing PC in its excited state (PC*) can donate an electron to the dormant chain-end bromide **A**, thus generating a propagating carbon radical **B** and the [PC$^{\bullet+}$][Br$^-$] complex. Upon vinyl addition of species **B** to the monomer, intermediate **C** is formed, which afterwards can undergo multiple pathways: (a) radical species may be recaptured by the [PC$^{\bullet+}$][Br$^-$] complex (**C** to **F**); (b) **C** may cyclize in a 5-*exo-trig* manner (**C** to **D**) or (c) a 6-*endo-trig* manner (**C** to **G**). Notably, the radical addition of **B** to the internal C–C double bond should be kinetically unfavorable due to its higher steric hindrance than the adjacent vinyl group. Finally, deactivation of radical species **D** and **G** by [PC$^{\bullet+}$][Br$^-$] results in the formation of dormant polymers **E** and **H**, respectively. Given the limited redox window of commonly used PCs, the resulting inactive alkyl chain-end bromide **H** is unlikely to be re-activated for propagation,[65] representing an unwanted pseudo-termination pathway. In this work, we report the synthesis of malonate-linked methacrylate-crotonate and *p*-toluenesulfonamide-linked acrylamide-crotonate monomers, and their highly selective radical cyclopolymerization by using a visible-light-driven photoredox ATRP approach.

Results and discussion

Initial radical cyclopolymerization of M1

To valid our hypothesis, **M1**, diethyl-2-bromo-2-methylmalonate (DBMM), and *N*,*N*′-di(2-naphthyl)dihydrophenazine

Open Access Article. Published on 21 February 2025. Downloaded on 1/23/2026 4:09:17 AM.
This article is licensed under a Creative Commons Attribution-NonCommercial 3.0 Unported Licence.

(**1**)[29] were selected as the monomer, initiator and photocatalyst, respectively. Gratifyingly, a 0.5 mmol-scale polymerization of **M1** under conditions of [**M1**]/[DBMM]/[**1**] = 500/10/1 in 1.0 mL of *N*,*N*-dimethylacetamide (DMAc), with white LED irradiation (~10.8 W) and a fan to maintain the temperature at ~30 °C, proceeded smoothly and reached 81% monomer conversion to give highly soluble **PM1** with a number-average molecular weight (M_n) of 8.7 kDa and a moderate dispersity ($Đ$) of 1.60 (Table 1, entry 1). The ^{1}H NMR spectrum of the obtained **PM1** (Fig. S44†) showed no signal of vinyl or alkenyl protons, suggesting an exclusive cyclopolymerizaton rather than the vinyl polymerization. As mentioned in Fig. 1c, cyclopentyl and cyclohexyl units are likely formed *via* 5-*exo-trig*- and 6-*endo-trig* cyclization, respectively. However, due to their high structural similarity, the ratios of these two units cannot be determined based on the ^{1}H NMR spectrum of **PM1**. Inspired by Niu's[56] and Huang's[66] strategy that utilizes a small-molecule model reaction to illustrate the structure of complex polymers, we performed a photoredox-catalyzed stoichiometric reaction of **M1** with a glycine derivative[67] as the radical precursor (Fig. 2). This reaction afforded the 5-membered product **2a** as a ~4 : 1 mixture of diastereomers in 44% yield, while its six-membered analogous product **2b** was not observed (Fig. S10 and 11†), indicating a favorable 5-*exo-trig* reaction pathway. Accordingly, the core structure of repeating units of the obtained **PM1** was ascertained as cyclopentane.

Effect of solvents, photocatalysts, and initiators

A brief screening of solvents (Table 1, entries 1–3) suggested that chlorobenzene (PhCl) was superior to others in achieving higher monomer conversion (92%) and producing **PM1** with a M_n (15.1 kDa) close to its theoretical value and a lower $Đ$ of 1.59 (entry 3). Replacing **PC1** with *N*,*N*′-di(4-CF_3-phenyl)dihydrophenazine (**PC2**) or core-modified *N*-(1-naphthyl)phenoxazine (**PC3**) led to slightly decreased monomer conversions and higher dispersity ($Đ$ = 1.64–1.70, entries 4 and 5). Examination of other commonly used O-ATRP alkyl bromide initiators, including ethyl α-bromophenylacetate (EBP) and methyl 2-bromopropionate (M2BP), revealed that DBMM outperformed these initiators, affording polymers with the best monomer conversion and dispersity (entries 6 and 7 *vs.* entry 3). Importantly, the radical cyclopolymerization did not proceed in the absence of light (entry 8), a PC (entry 8), or an initiator (entry 10), providing strong evidence for the photoredox ATRP mechanism. Additionally, polymerization performed with [**M1**]/[DBMM]/[**1**] = 500/25/1 produced **PM1** with predictable M_n = 7.2 kDa and moderate $Đ$ = 1.59 (entry 11), while attempts to target higher degree of polymerization (DP) were unsuccessful (entries 12 and 13), probably due to increased termination events.

Investigation of the role of light intensity

Compared to typical O-ATRP, which produces well-defined poly(methacrylates) with $Đ$ < 1.2, this photoredox radical cyclopolymerization of **M1** generally afforded **PM1** with $Đ$ ~ 1.6. This higher dispersity is likely due to the incorporation of the crotonate moiety, which introduces a secondary radical species that is structurally similar to the propagating radical in the ATRP of acrylates. Since the propagating rate constant (k_p) of acrylates is an order of magnitude higher than that for methacrylates,[68]

Table 1 Photocontrolled radical cyclopolymerization of **M1**[a]

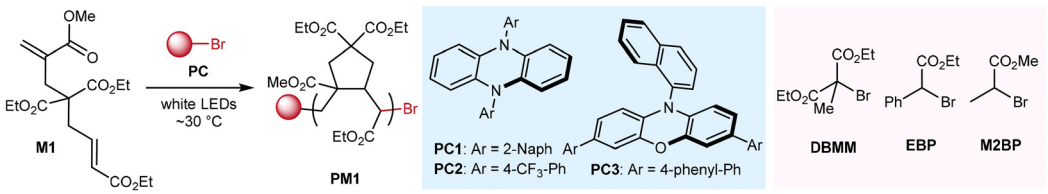

Entry	PC	Initiator	[**M1**]/[**I**]/[**PC**]	Solvent	Conv.[b] (%)	$M_{n,theo}$[c] (kDa)	M_n[d] (kDa)	$Đ$[d]
1	**PC1**	DBMM	500/10/1	DMAc	81	15.2	8.7	1.60
2	**PC1**	DBMM	500/10/1	EtOAc	91	16.9	14.6	1.85
3	**PC1**	DBMM	500/10/1	PhCl	92	17.3	15.1	1.59
4	**PC2**	DBMM	500/10/1	PhCl	85	16.0	15.7	1.70
5	**PC3**	DBMM	500/10/1	PhCl	89	16.7	12.7	1.64
6	**PC1**	EBP	500/10/1	PhCl	76	14.3	12.4	1.60
7	**PC1**	M2BP	500/10/1	PhCl	64	12.0	11.3	1.66
8[e]	**PC1**	DBMM	500/10/1	PhCl	0	—	—	—
9	—	DBMM	500/10/1	PhCl	0	—	—	—
10	**PC1**	—	500/10/1	PhCl	0	—	—	—
11	**PC1**	DBMM	500/25/1	PhCl	96	7.4	7.2	1.59
12	**PC1**	DBMM	1000/10/1	PhCl	71	26.5	15.4	1.68
13	**PC1**	DBMM	2000/10/1	PhCl	38	28.3	13.2	1.63

[a] Polymerizations performed using 0.5 mmol of **M1**, 0.0025–0.025 mmol of alkyl bromide, 0.001 mmol of PC, 1.0 mL of solvent, and irradiated with white LEDs (~10.8 W) for 12 h. A cooling fan was used to maintain the temperature at ~30 °C. [b] Measured by crude ^{1}H-NMR. [c] $M_{n,theo}$ = MW(initiator) + MW(**M1**) × conversion × ([**M1**]/[initiator]). [d] Determined by gel permeation chromatography (GPC) in THF (1.0 mL min^{-1}, 40 °C) and calibrated with polystyrene standards. [e] In the dark.

 This journal is © The Royal Society of Chemistry 2025

Open Access Article. Published on 21 February 2025. Downloaded on 1/23/2026 4:09:17 AM.
This article is licensed under a Creative Commons Attribution-NonCommercial 3.0 Unported Licence.

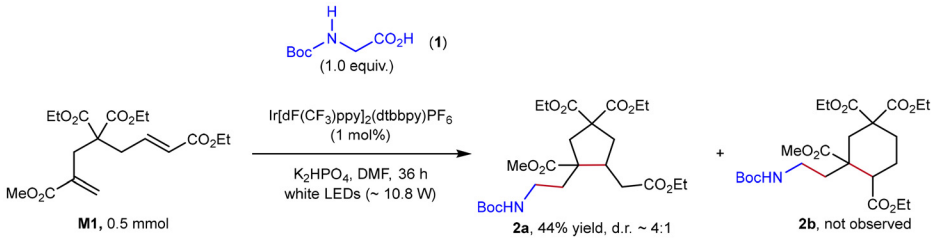

Fig. 2 Model reaction of **M1** with glycine derivative **2** under photoredox conditions.

the chain growth through crotonate-to-methacrylate cross propagation is challenging to control. In addition, the occasional formation of six-membered cyclic repeating units (**C** to **G** to **H**, Fig. 1c) likely contributes to chain termination, further complicating the control of polymer chain growth.

To gain deeper insights into the overall control of the polymerization, several experiments were performed. First, the role of light intensity in the polymerization of [**M1**]/[DBMM]/[**1**] = 500/10/1 in PhCl at ~30 °C was investigated. In fact, first-order kinetics were revealed for polymerizations conducted under white LED irradiation ranging from 1.4 to 10.8 W (Fig. 3a). The rates of polymerization roughly correlated to the intensity of irradiation and decreased with lower light intensity, as it actually influences the concentration of the excited-state PC,[69] which in turn regulates the radical cyclopolymerization. Importantly, two **PM1** samples, synthesized under 10.8 W (Fig. 3b) and 1.4 W irradiation (Fig. 3c), were analyzed by matrix-assisted laser desorption ionization time of flight mass (MALDI-TOF MS) spectrometry. The analyses revealed that increased light intensity can accelerate side reactions, such as radical coupling and hydrogen atom abstraction to form a C–H chain end.

Kinetic study and chain-end fidelity

We then monitored the polymerization of [**M1**]/[DBMM]/[**PC1**] = 500/10/1 in PhCl (0.5 M) at ~30 °C, with 1.4 W white LED irradiation. First, a linear increase in polymer MW as a function of monomer conversion was observed (Fig. 4a), demonstrating the robustness of the O-ATRP process. Second, a pulsed irradiation experiment was performed, where the cyclopolymerization proceeded with light, paused in the dark, and revived upon re-irradiation (Fig. 4b and c). Third, the excellent chain-end fidelity allowed chain extension with methyl methacrylate (MMA) using the isolated **PM1** (M_n = 4.9 kDa, $Đ$ = 1.60) as the macroinitiator (Fig. 4d). The gel-permeation chromatography (GPC) traces before and after the chain extension confirmed the successful preparation of the block copolymer **PM1**-*b*-**PMMA** (Fig. 4e).

Effect of bromide additives

From the perspective of the reversible-deactivation mechanism in ATRP, the addition of bromide salts primarily shifts the equilibrium to the dormant Br chain ends, thereby enhancing control over the polymer chain growth.[35] We investigated the effects of LiBr on cyclopolymerization of [**M1**]/[DBMM]/[**1**] = 500/10/1 in PhCl at ~30 °C under ~1.4 W white LED irradiation (Table 2, entries 1–3). The inclusion of LiBr, regardless of its concentration, unexpectedly led to an increase in dispersity, probably due to its poor solubility in PhCl. In polymerizations of **M1** performed in EtOAc, the polymerization rates were negatively correlated to the concentration of LiBr, although the dispersities of the obtained **PM1** remained high (entries 4–6). We then turned to tetrabutylammonium bromide (TBAB) as an additive. Encouragingly, despite a reduction in monomer conversion, the addition of 3.0 equiv. of TBAB to DBMM resulted in the formation of **PM1** with a M_n of 11.8 kDa and a low $Đ$ of 1.38 (entry 9). More importantly, the MALDI-TOF MS analysis of low molecular-weight **PM1** synthesized under such conditions (entry 9) indicated high chain-

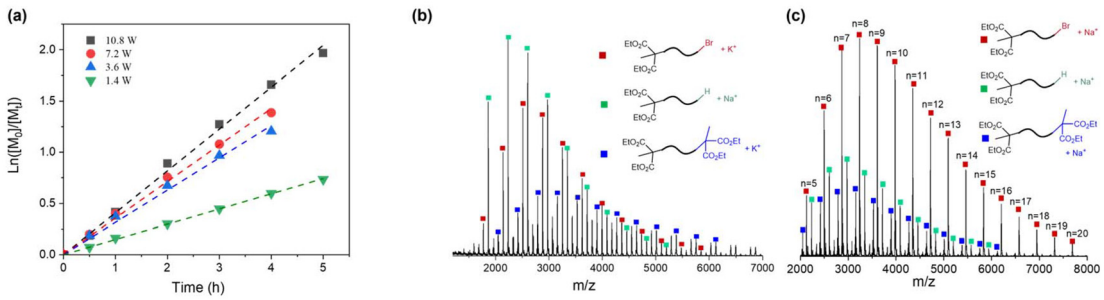

Fig. 3 (a) Plots of natural log of monomer conversion as a function of time for polymerization of [**M1**]/[DBMM]/[**PC1**] = 500/10/1 performed in PhCl (0.5 M), at ~30 °C, with 1.4–10.8 W white LED irradiation. MALDI-TOF MS spectra of low-MW **PM1** synthesized with (b) 10.5 W and (c) 1.4 W white LED irradiation.

Open Access Article. Published on 21 February 2025. Downloaded on 1/23/2026 4:09:17 AM.
This article is licensed under a Creative Commons Attribution-NonCommercial 3.0 Unported Licence.

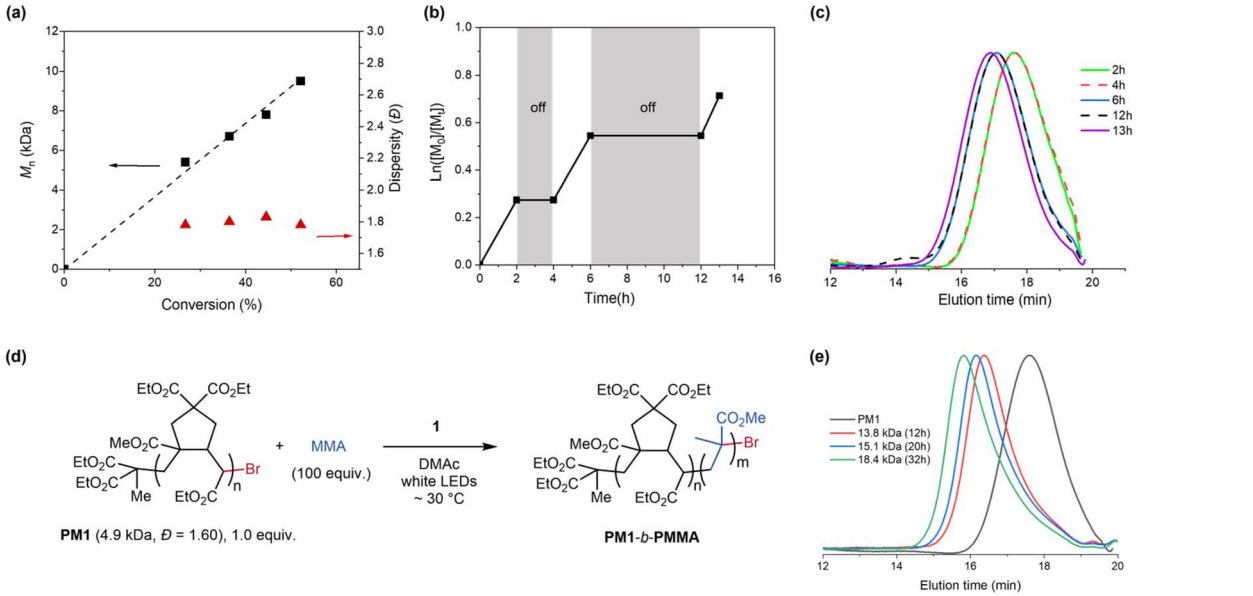

Fig. 4 (a) Plots of measured M_n and $Đ$ as a function of monomer conversion for polymerization of [**M1**]/[DBMM]/[**PC1**] = 500/10/1 performed in PhCl (0.5 M), at ~30 °C, with 1.4 W white LED irradiation. (b) Plots of natural log of monomer conversion as a function of time and (c) overlaid GPC traces for the pulsed irradiation experiment. (d) Chain-extension polymerization from a **PM1** macroinitiator with MMA. (e) Overlayed GPC traces for chain-extension polymerization.

Table 2 Effect of bromide additives on photoredox radical cyclopolymerization of **M1** [a]

Entry	Additive	Solvent	[**M1**]/[DBMM]/[**1**][**Br**]	Conv.[b] (%)	$M_{n,theo}$[c] (kDa)	M_n[d] (kDa)	$Đ$[d]
1	LiBr	PhCl	500/10/1/10	79	14.9	13.4	1.91
2	LiBr	PhCl	500/10/1/20	77	14.5	11.9	1.90
3	LiBr	PhCl	500/10/1/30	76	14.3	12.1	1.97
4	LiBr	EtOAc	500/10/1/10	77	14.5	11.8	1.79
5	LiBr	EtOAc	500/10/1/20	65	12.3	7.5	1.95
6	LiBr	EtOAc	500/10/1/30	55	10.4	7.4	1.96
7	TBAB	PhCl	500/10/1/10	79	14.9	15.1	1.59
8	TBAB	PhCl	500/10/1/20	85	16.0	13.6	1.48
9	TBAB	PhCl	500/10/1/30	68	12.8	11.8	1.38

[a] Polymerizations performed using 0.5 mmol of **M1**, 0.01 mmol of DBMM, 0.001 mmol of **1**, 0.01–0.03 mmol of bromide additive, 1.0 mL of PhCl, and irradiated with white LEDs (~1.4 W) for 12 h. A cooling fan was used to maintain the temperature at ~30 °C. [b] Measured by crude ^{1}H-NMR. [c] $M_{n,theo}$ = MW(initiator) + MW(**M1**) × conversion × ([**M1**]/[initiator]). [d] Determined by gel permeation chromatography (GPC) in THF (1.0 mL min^{-1}, 40 °C) and calibrated with polystyrene standards.

end fidelity (Fig. S3†), underscoring the importance of the bromide anion in the photoredox deactivation process.

Scope of methacrylate-crotonate diene monomers

With the optimized conditions in hand, we next explored the generality of this radical cyclopolymerization method (Fig. 5). Diene monomers containing methyl- (**M2**), benzyl- (**M3**), and *tert*-butyl crotonate (**M4**) motifs were successfully polymerized by using this organocatalyzed photoredox protocol, affording the corresponding **PM2–PM4** of 10.3–17.2 kDa and with moderate dispersities of ~1.5. It is noteworthy that the monomer structure significantly impacts the polymerizability. First, the substituent effect of the crotonate motif was observed. Compared to **M2** and **M3**, **M4** bearing a sterically bulky *tert*-butyl group exhibited lower reactivity under identical polymerization conditions, as evidenced by lower monomer conversion (80%). Second, the linker's chemical structure principally dominates the monomer's cyclopolymerizability. For instance, polymerization of **M5**, which contains a cyanoacetate linkage, proceeded more slowly, reaching only 45% conversion to produce **PM5** with M_n = 4.5 kDa and $Đ$ = 1.58. In contrast, polymerizations of *p*-toluenesulfonamide-linked **M6** and acrylamide-crotonate monomer **M7** achieved near quantitative conversions, yielding **PM6** (M_n = 7.1 kDa and $Đ$ = 1.66) and **PM7** (M_n = 22.2 kDa and $Đ$ = 1.80), respectively. Finally, the block copolymer **PM1**-*b*-**PM6** (M_n = 12.0 kDa and $Đ$ = 1.57) was successfully synthesized using **PM1** (M_n = 5.3 kDa and $Đ$ = 1.71) as the macroinitiator and **M6** as the comonomer, as evidenced by the shift of retention time in the GPC traces before and after the copolymerization (Fig. S9†).

This journal is © The Royal Society of Chemistry 2025

Open Access Article. Published on 21 February 2025. Downloaded on 1/23/2026 4:09:17 AM.
This article is licensed under a Creative Commons Attribution-NonCommercial 3.0 Unported Licence.

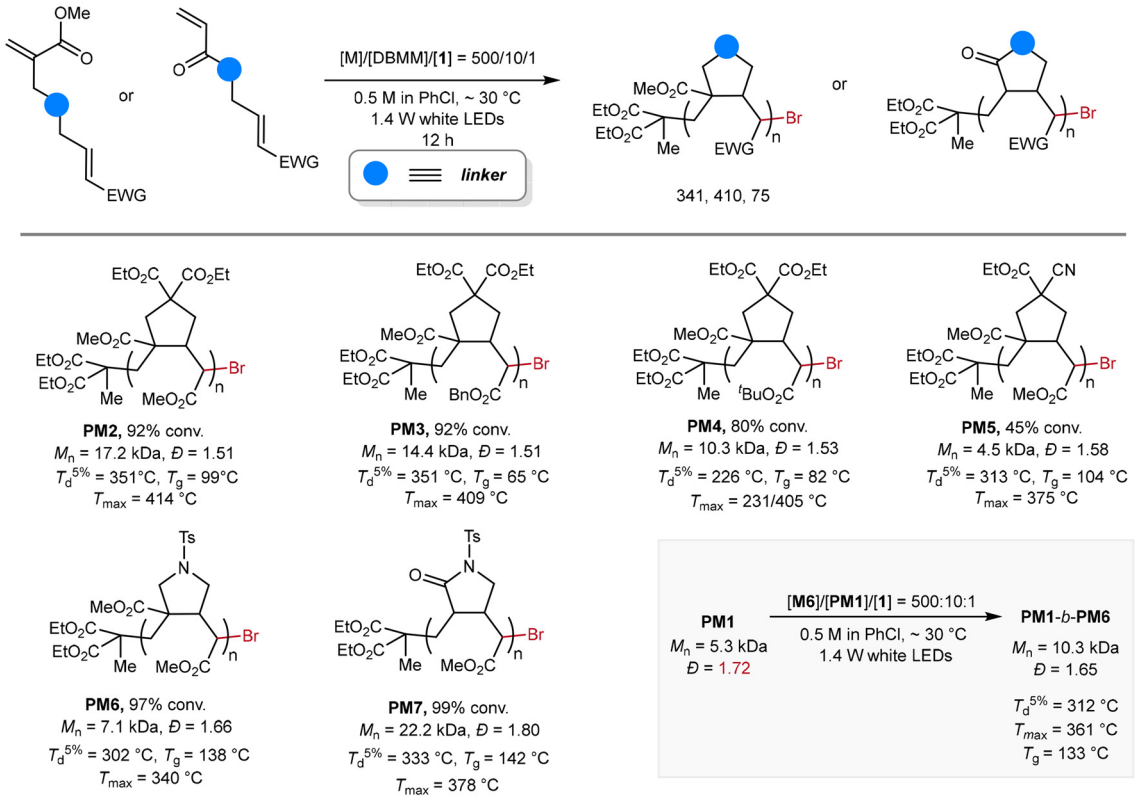

Fig. 5 Monomer scope.

The thermal properties of the obtained polymers were then investigated. First, the thermal stability of **PM1–PM7** was examined by thermogravimetric analysis (TGA) in terms of decomposition temperature at 5% weight loss ($T_d^{5\%}$) and maximum decomposition temperature (T_{max}), which is defined as the peak value in relative derivative thermogravimetry (DTG). **PM1–PM3** generally exhibited high $T_d^{5\%}$ of 314–351 °C and T_{max} of 409–410 °C, while those of **PM4** significantly decreased to 226 °C and 231 °C, respectively, probably due to the fast decomposition of the pendent *tert*-butyl group. Nitrogen-containing polymers, **PM5–PM7**, seem to be less stable in terms of lower $T_d^{5\%}$ (302–333 °C) and T_{max} (340–378 °C). Second, the glass transition temperatures (T_gs) of **PM1–PM4** were measured by differential scanning calorimetry (DSC), ranging from 65 to 99 °C. The T_gs of nitrogen-containing **PM5–PM7** (104 to 142 °C) are higher than those for polymers bearing cyclopentane units, indicating the presence of more rigid cyclic structures.

Experimental

Materials and methods

All chemicals were purchased from TCI, J&K, Energy Chemical, and Adamas-beta, and were used as received without further purification. All syntheses and handling of air- and moisture-sensitive chemicals were performed in a N_2-filled glove box.

^{1}H NMR and ^{13}C NMR spectroscopy

^{1}H NMR and ^{13}C NMR spectra were recorded on a Bruker 400 Hz (100 Hz for ^{13}C) spectrometer at ambient temperature. Chemical shifts (δ) for both ^{1}H and ^{13}C NMR spectra are given in ppm relative to tetramethylsilane. All NMR spectra were referenced to the residual solvent ($CHCl_3$) signal (δ = 7.26 ppm for ^{1}H NMR and δ = 77.00 ppm for ^{13}H NMR).

Gel permeation chromatography (GPC)

Analysis of polymers' number-average molecular weight (M_n) and dispersity ($Đ$) was performed using a Waters e2695 system (with one guard column and two Styragel columns) coupled with a Waters 2414 refractive index detector (calibrated with 10 polystyrene standards). The analysis was performed at 40 °C using THF as the eluent at a flow rate of 1.0 mL per minute.

Thermo-gravimetric analysis (TGA)

Decomposition temperatures ($T_d^{5\%}$) at 5% weight loss and maximum rate decomposition temperatures (T_{max}) of the obtained polymers were measured by thermal gravimetric analysis (TGA) on a TA Q50 analyzer, TA instruments. Polymer samples were measured by heating the polymer samples from 25 °C to 700 °C at the rate of 10 °C min^{-1}.

Open Access Article. Published on 21 February 2025. Downloaded on 1/23/2026 4:09:17 AM.
This article is licensed under a Creative Commons Attribution-NonCommercial 3.0 Unported Licence.

Differential scanning calorimetry (DSC)

Glass transition temperatures (T_g) of the obtained polymers were measured by differential scanning calorimetry (DSC) on a TA Q20 analyzer, at a rate of 10 °C min^{-1}. All T_g values were obtained from a second scan.

Conclusions

In summary, we have designed and synthesized a series of diene monomers that integrate methacrylates or acrylamide with crotonates. By using *N*,*N*′-di(2-naphthyl)dihydrophenazine **1** as the photocatalyst and DBMM as the initiator, radical polymerization of these hybrid monomers proceeded exclusively through a sequence of intramolecular cyclization and intermolecular propagation, resulting in polymers with unique cyclic repeating units. Kinetic studies, along with the effects of light intensity and bromide additives, combined with MALDI-TOF mass spectrometry analysis, have provided valuable insights into this radical cyclopolymerization driven by the photoredox ATRP mechanism. This approach enables straightforward synthesis of a range of novel homopolymers and block copolymers with low to moderate dispersities. With these findings presented in this work, we believe that photocontrolled radical cyclopolymerization is a promising and practical strategy for accessing new polymeric materials with distinct properties.

Author contributions

G.-Y. and Y.-L. T. performed the experiments. G.-Y., Y.-L. T. and K. L. analyzed the data. D.-F. C. directed the project and wrote the manuscript with assistance from all authors. G.-Y. and Y.-L. T. contributed equally to this work.

Data availability

The data supporting this article have been included as part of the ESI.†

Conflicts of interest

The authors declare no competing financial interest.

Acknowledgements

This work was financially supported by the NSFC (grant no. 22101273) and the Fundamental Research Fund for the Central Universities (WK9990000111). This work was partially carried out at the Instruments Center for Physical Science, University of Science and Technology of China (USTC).

References

1 F. A. Leibfarth, K. M. Mattson, B. P. Fors, H. A. Collins and C. J. Hawker, *Angew. Chem., Int. Ed.*, 2013, **52**, 199–210.
2 X. Pan, M. A. Tasdelen, J. Laun, T. Junkers, Y. Yagc and K. Matyjaszewski, *Prog. Polym. Sci.*, 2016, **62**, 73–125.
3 M. Chen, M. Zhong and J. A. Johnson, *Chem. Rev.*, 2016, **116**, 10167–10211.
4 S. Dadashi-Silab, S. Droan and Y. Yagci, *Chem. Rev.*, 2016, **116**, 10212–10275.
5 N. Corrigan, S. Shanmugam, J. Xu and C. Boyer, *Chem. Soc. Rev.*, 2016, **45**, 6165–6212.
6 D. A. Corbin and G. M. Miyake, *Chem. Rev.*, 2022, **122**, 1830–1874.
7 Q. Michaudel, V. Kottisch and B. P. Fors, *Angew. Chem., Int. Ed.*, 2017, **56**, 9670–9679.
8 Y. Zhou, J. Li, Y. Wu and Z. Luo, *Chem. Rev.*, 2020, **120**, 2950–3048.
9 J. E. Poelma, B. P. Fors, G. F. Meyers, J. W. Kramer and C. J. Hawker, *Angew. Chem., Int. Ed.*, 2013, **52**, 6844–6848.
10 C. W. Pester, B. Narupai, K. M. Mattson, D. P. Bothman, D. Klinger, K. W. Lee, E. H. Discekici and C. J. Hawker, *Adv. Mater.*, 2016, **28**, 9292–9300.
11 E. H. Discekici, C. W. Pester, N. J. Treat, J. Lawrence, K. M. Mattson, B. Narupai, E. P. Toumayan, Y. Luo, A. J. McGrath, P. G. Clark, J. Read de Alaniz and C. J. Hawker, *ACS Macro Lett.*, 2016, **5**, 258–262.
12 J. Yan, X. Pan, M. Schmitt, Z. Wang, M. R. Bockstaller and K. Matyjaszewski, *ACS Macro Lett.*, 2016, **5**, 661–665.
13 E. H. Discekici, A. Anastasaki, J. Read De Alaniz and C. J. Hawker, *Macromolecules*, 2018, **51**, 7421–7434.
14 J.-S. Wang and K. Matyjaszewski, *J. Am. Chem. Soc.*, 1995, **117**, 5614–5615.
15 M. Kato, M. Kamigaito, M. Sawamoto and T. Higashimura, *Macromolecules*, 1995, **28**, 1721–1723.
16 D. Konkolewicz, K. Schroder, J. Buback, S. Bernhard and K. Matyjaszewski, *ACS Macro Lett.*, 2012, **1**, 1219–1223.
17 J. Mosnáček and M. Ilčíková, *Macromolecules*, 2012, **45**, 5859–5865.
18 A. Anastasaki, V. Nikolaou, Q. Zhang, J. Burns, S. R. Samanta, C. Waldron, A. J. Haddleton, R. McHale, D. Fox, V. Percec, P. Wilson and D. M. Haddleton, *J. Am. Chem. Soc.*, 2014, **136**, 1141–1149.
19 B. P. Fors and C. J. Hawker, *Angew. Chem., Int. Ed.*, 2012, **51**, 8850–8853.
20 X. Pan, N. Malhotra, J. Zhang and K. Matyjaszewski, *Macromolecules*, 2015, **48**, 6948–6954.
21 S. Dadashi-Silab, X. Pan and K. Matyjaszewski, *Macromolecules*, 2017, **50**, 7967–7977.
22 K. Parkatzidis, S. Boner, H. S. Wang and A. Anastasaki, *ACS Macro Lett.*, 2022, **11**, 841–846.
23 G. M. Miyake and J. C. Theriot, *Macromolecules*, 2014, **47**, 8255–8261.
24 C. Aydogan, G. Yilmaz and Y. Yagci, *Macromolecules*, 2017, **50**, 9115–9120.

 This journal is © The Royal Society of Chemistry 2025

Open Access Article. Published on 21 February 2025. Downloaded on 1/23/2026 4:09:17 AM. This article is licensed under a Creative Commons Attribution-NonCommercial 3.0 Unported Licence.

25 N. J. Treat, H. Sprafke, J. W. Kramer, P. G. Clark, B. E. Barton, J. Read de Alaniz, B. P. Fors and C. J. Hawker, *J. Am. Chem. Soc.*, 2014, **136**, 16096–16101.
26 X. Pan, M. Lamson, J. Yan and K. Matyjaszewski, *ACS Macro Lett.*, 2015, **4**, 192–196.
27 Y. C. Zhao, H. H. Gong, K. M. Jiang, S. J. Yan, J. Lin and M. Chen, *Macromolecules*, 2018, **51**, 938–946.
28 H. Zhou, L. Zhang, P. Wen, Y. Zhou, Y. Zhao, Q. Zhao, Y. Gu, R. Bai and M. Chen, *Angew. Chem., Int. Ed.*, 2023, **62**, e202304461.
29 J. Theriot, C.-H. Lim, H. Yang, M. Ryan, C. Musgrave and G. Miyake, *Science*, 2016, **352**, 1082–1086.
30 C.-H. Lim, M. D. Ryan, B. G. McCarthy, J. C. Theriot, S. M. Sartor, N. H. Damrauer, C. B. Musgrave and G. M. Miyake, *J. Am. Chem. Soc.*, 2017, **139**, 348–355.
31 R. M. Pearson, C.-H. Lim, B. G. McCarthy, C. B. Musgrave and G. M. Miyake, *J. Am. Chem. Soc.*, 2016, **138**, 11399–11407.
32 B. G. McCarthy, R. M. Pearson, C. H. Lim, S. M. Sartor, N. H. Damrauer and G. M. Miyake, *J. Am. Chem. Soc.*, 2018, **140**, 5088–5101.
33 V. K. Singh, C. Yu, S. Badgujar, Y. Kim, Y. Kwon, D. Kim, J. Lee, T. Akhter, G. Thangavel and L. S. Park, *Nat. Catal.*, 2018, **1**, 794–804.
34 C. Kutahya, A. Allushi, R. Isci, J. Kreutzer, T. Ozturk, G. Yilmaz and Y. Yagci, *Macromolecules*, 2017, **50**, 6903–6910.
35 B. L. Buss, C. H. Lim and G. M. Miyake, *Angew. Chem., Int. Ed.*, 2020, **59**, 3209–3217.
36 Q. Ma, J. Song, X. Zhang, Y. Jiang, L. Ji and S. Liao, *Nat. Commun.*, 2021, **12**, 429.
37 H. Shao, S. Li, Y. Jiang, J. Song, X. Zhang, J. Chen and S. Liao, *Polym. Chem.*, 2024, **15**, 4134–4140.
38 B. McCarthy, S. Sartor, J. Cole, N. Damrauer and G. M. Miyake, *Macromolecules*, 2020, **53**, 9208–9219.
39 C. Aydogan, C. Kutahya, A. Allushi, G. Yilmaz and Y. Yagci, *Polym. Chem.*, 2017, **8**, 2899–2903.
40 Y. Xu, G. Li, Y. Hu and Y. Wang, *Macromol. Chem. Phys.*, 2018, **219**, 1800192.
41 D. Wei, Y. Xu, C. Liu, Y. Zhai, H. Chen, L. Bai, H. Yang, L. Yang, W. Wang and Y. Niu, *J. Polym. Sci., Part A: Polym. Chem.*, 2019, **57**, 1265–1269.
42 J. S. Yuan, W. Q. Wang, Z. F. Zhou and J. Niu, *Macromolecules*, 2020, **53**, 5655–5673.
43 G. I. Peterson and T. L. Choi, *Chem. Sci.*, 2020, **11**, 4843–4854.
44 G. Chen, L. Xia, F. Wang, Z. Zhang and Y.-Z. You, *Polym. Chem.*, 2021, **12**, 3740–3752.
45 D.-Y. Zhang and D.-F. Chen, *J. Funct. Polym.*, 2023, **36**, 261–274.
46 D. Pasini and D. Takeuchi, *Chem. Rev.*, 2018, **118**, 8983–9057.
47 G. B. Butler and R. J. Angelo, *J. Am. Chem. Soc.*, 1957, **79**, 3128–3131.
48 Y. Kametani, M. Nakano, T. Yamamoto, M. Ouchi and M. Sawamoto, *ACS Macro Lett.*, 2017, **6**, 754–757.
49 P. Gerdt and A. Studer, *Angew. Chem., Int. Ed.*, 2022, **61**, e202206964.
50 Y. Assem, H. Chaffey-Millar, C. Barner-Kowollik, G. Wegner and S. Agarwal, *Macromolecules*, 2007, **40**, 3907–3913.
51 Y. Assem, A. Greiner and S. Agarwal, *Macromol. Rapid Commun.*, 2007, **28**, 1923–1928.
52 S. Erkoc and A. E. Ouchi, *Macromolecules*, 2008, **41**, 9019–9024.
53 J. Li, M. Du, Z. Zhao and H. Liu, *Macromolecules*, 2016, **49**, 445–454.
54 Y. Kametani, M. Sawamoto and M. Ouchi, *Angew. Chem., Int. Ed.*, 2018, **57**, 10905–10909.
55 Y. Kametani, F. Tournilhac, M. Sawamoto and M. Ouchi, *Angew. Chem., Int. Ed.*, 2020, **59**, 5193–5201.
56 H. Huang, W. Wang, Z. Zhou, B. Sun, M. An, F. Haeffner and J. Niu, *J. Am. Chem. Soc.*, 2019, **141**, 12493–12497.
57 Y. Wang, J. Du and H. Huang, *Angew. Chem., Int. Ed.*, 2024, **63**, e202318898.
58 M. Tsuji, R. Sakai, T. Satoh, H. Kaga and T. Kakuchi, *Macromolecules*, 2002, **35**, 8255–8257.
59 S. Erkoc, L. J. Mathias and A. E. Acar, *Macromolecules*, 2006, **39**, 8936–8942.
60 Y. Hibi, M. Ouchi and M. Sawamoto, *Angew. Chem., Int. Ed.*, 2011, **50**, 7434–7437.
61 M. Ouchi, M. Nakano, T. Nakanishi and M. Sawamoto, *Angew. Chem., Int. Ed.*, 2016, **55**, 14584–14589.
62 Y. Hibi, S. Tokuoka, T. Terashima, M. Ouchi and M. Sawamoto, *Polym. Chem.*, 2011, **2**, 341–347.
63 Z. Hu, Y.-P. Xu, D. Wu, B. Li, Y.-C. Huang, J.-X. Jiang, G.-Q. Lai and T.-Y. Luh, *Macromol. Chem. Phys.*, 2012, **213**, 566–571.
64 S. Moins, J. C. Martins, A. Krumpmann, V. Lemaur, J. Cornil, N. Delbosc, A. Decroly, P. Dubois, R. Lazzaroni, J.-F. Gohy and O. Coulembier, *Chem. Commun.*, 2017, **53**, 6899–6902.
65 D.-F. Chen, B. M. Boyle, B. G. McCarthy, C.-H. Lim and G. M. Miyake, *J. Am. Chem. Soc.*, 2019, **141**, 13268–13277.
66 S. Zhang, C. Cao, S. Jiang and H. Huang, *Macromolecules*, 2022, **55**, 9411–9419.
67 L. Chu, C. Ohta, Z. Zuo and D. W. C. MacMillan, *J. Am. Chem. Soc.*, 2014, **136**, 10886–10889.
68 W. Tang and K. Matyjaszewski, *Macromolecules*, 2007, **40**, 1858–1863.
69 M. D. Ryan, R. M. Pearson, T. A. French and G. M. Miyake, *Macromolecules*, 2017, **50**, 4616–4622.